Supporting Information

The Preparation of Zero Valence Pd Nanoparticles with Ultra Efficient electrocatalytic activity for ORR

Wenyan Si, [a, c] ‡ Ze Yang, [a] ‡ Xiuli Hu, [a] Qing Lv,* [b] Xiaodong Li, [a, c] Fuhua Zhao, [a] Jianjiang He, [a] and Changshui Huang* [a]

[a] Qingdao Institute of Bioenergy and Bioprocess Technology Chinese Academy of Sciences, Qingdao 266101, China

[b] School of Chemistry and Chemical Engineering, Shandong University, Shandong 250100, China

[c] Center of Materials Science and Optoelectronics Engineering, University of Chinese Academy of Sciences, Beijing 100049, China

1. Method of ECSA testing.

The ECSA was calculated using CO stripping voltammograms. In detail, CO was bubbled in the 0.5 M H_2SO_4 electrolyte for 20 minutes at a constant potential of 0.1 V vs. SCE. Then Ar was used to purge out the excess CO in the electrolyte for 25 minutes. After that, 3 cycles of CVs were measured at a potential range of -0.242-0.958 V vs. SCE. The ESCA was determined according to the peak area of CO oxidation with the following formula.

$$ECSA = \frac{[S_{CO} / v]}{0.42 * M_{Pd}}$$

2. Electrochemical evaluation in acidic media.

The ORR performances of the Pd/N-HsGY catalysts in acidic media were measured in 0.1 M $HClO_4$ solution. The LSV curves of all kinds of tested catalysts (Figure S20a) indicate that Pd/N-HsGY shows the best catalytic activity among them. The half-wave potential of Pd/N-HsGY is 0.79 V vs. RHE, much higher than that of

commercial Pt/C (0.72 V vs. RHE) and Pd/C (0.67 V vs. RHE) (Figure S20a), which determines the higher activity of Pd/N-HsGY than commercial Pt/C and Pd/C. Figures S18-19 display the mass activities and specific activities of the samples in acidic media. The mass activity of Pd/N-HsGY is 0.195 A mg^{-1}_{Pd} at 0.8 V (vs RHE), which is much higher than Pt/C (0.035 A mg^{-1}_{Pt}) and Pd/C (0.011 A mg^{-1}_{Pd}). As shown in Figure S20c, the specific activity of Pd/N-HsGY is 0.908 mA cm^{-2}_{Pd} at 0.8 V (vs RHE), which was 18.6 times higher than Pt/C (0.043 mA cm^{-2}_{Pt}) and ca. 100 times higher than Pd/C (0.009 mA cm^{-2}_{Pd}). The excellent activity of Pd/N-HsGY-1000 should derive from the synergistic effect of HsGY, Pd and the doped N.

The stability of the catalysts was measured by comparing the LSVs before and after cyclic voltammetry (CV) in O_2-saturated $HClO_4$ for 5000 cycles. The half-wave potential of Pd/N-HsGY was negatively shifted by 29 mV, much smaller than that of Pt/C (71 mV) (Figure S21a, b), which means Pd/N-HsGY was more stable than Pt/C. The methanol tolerance of the catalysts was tested by LSV curves of Pd/N-HsGY and commercial Pt/C before and after injecting methanol into O_2-saturated 0.1 M $HClO_4$ at 1600 rpm. Figure S22a and b show that the activity of Pd/N-HsGY was affected much less by methanol than Pt/C. The electron transfer number of Pd/N-HsGY were calculated by K-L equation and RRDE test, the value was above 3.93 and the yield of peroxide is below 6% (Figure S23b), showing that ORR mainly occurs by a four-electron transfer pathway on Pd/N-HsGY in acidic medium.

3. Theory Calculation

All density functional theory (DFT) calculations are performed in the Vienna Ab Initio Simulation Package (VASP) code based on the projector augmented wave (PAW) approach.[1-2] The Perdew–Burke–Ernzerhof (PBE) functional is chosen here to describe the exchange-correlation interactions. The plane-wave cutoff energy of 500 eV is used, and the energies and residual forces are converged to 10^{-6} eV and 0.02 eV $Å^{-1}$ in the process of electronic and geometric optimizations. In our calculation, the optimized HsGY lattice parameters are $\alpha = \beta = 90°$ and $\gamma = 120°$; a = b = 16.4050 Å and the

vacuum distance is 20 Å in the c-axis. During optimization of HsGY systems, the K-point grid is set to 3 x 3 x 1. The adsorption energy of Pd/HsGY is calculated with the following formula: $E_{ads} = E_{Pd/HsGY} - E_{HsGY} - E_{Pd}$, where $E_{pd/HsGY}$, E_{HsGY} and E_{pd} are the energies of Pd/HsGY, HsGY and Pd nanoparticles, respectively;[3] To analyze the stability of Pd nano-clusters adsorb on N doped HsGY, the adsorption energy of Pd/N-HsGY is also calculated.

Additionally, the ORR reaction pathway of Pd or PdO nanoparticles, Pd/HsGY and Pd/N-HsGY systems are calculated.[4] The Pd nanoparticle is mimicked by a cluster containing 13 Pd atoms while PdO is mimicked by a cluster containing 18 Pd atoms and 18 O atoms. Spin-polarization was considered for all calculations. The reactions of the complete 4e ORR in an acidic medium used in the free energy profiles calculation are:

$* + O_2(g) + H^+ + e^- \rightarrow *OOH$

$*OOH + H^+ + e^- \rightarrow *O + H_2O(l)$

$*O + H^+ + e^- \rightarrow *OH$

$*OH + H^+ + e^- \rightarrow * + H_2O(l)$

While the reactions of the complete 4e ORR in an alkaline medium used in the free energy profiles calculation are:

$* + O_2(g) + H_2O(l) + e^- \rightarrow *OOH + OH^-$

$*OOH + e^- \rightarrow *O + OH^-$

$*O + H_2O(l) + e^- \rightarrow *OH + OH^-$

$*OH + e^- \rightarrow * + OH^-$

where * denotes the active site, *OOH, *O, and *OH represent the oxygen-containing intermediates.[4]

The Gibbs free energy change (ΔG) is calculated according to $\Delta G = \Delta E_{DFT} + \Delta E_{ZPE} -$

$T\Delta S+\Delta Gu$, Where E_{DFT} is the total energy obtained from DFT, E_{ZPE} is the in zero point energy, T is temperature and S is the entropy. ΔGu = -eU, where e is the transferred charge and U is the electrode potential with respect to standard hydrogen electrode. Gas phase H_2O at 0.035 bar was used as the reference state, since at this pressure, the gas-phase H_2O is in equilibrium with liquid water at 298.15 K. The Gibbs free energy of O_2 is derived as $G(O_2(g)) = 2G(H_2O(l)-2G(H_2(g))+4.92$ eV and the Gibbs free energy of H^+ in solution is estimated by $1/2G(H_2)$.

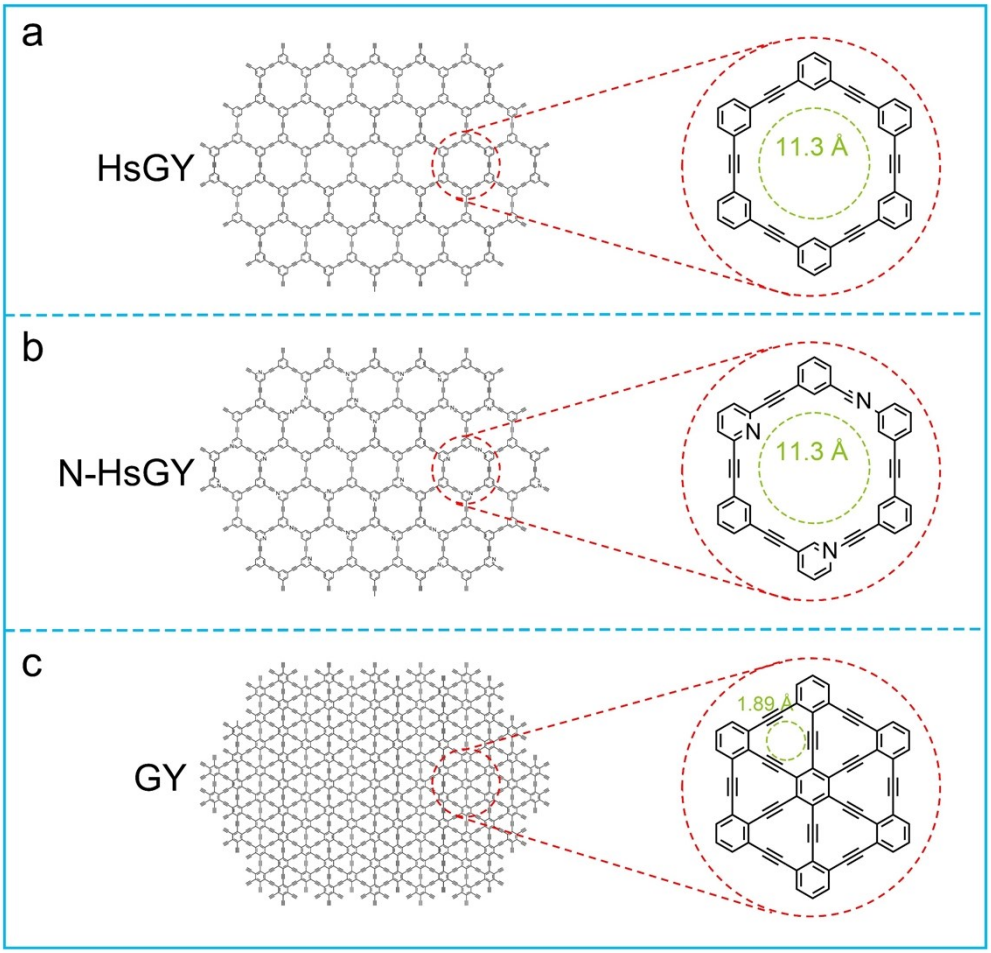

Figure S1. The structure of (a) HsGY, (b) N-HsGY and (c) GY.

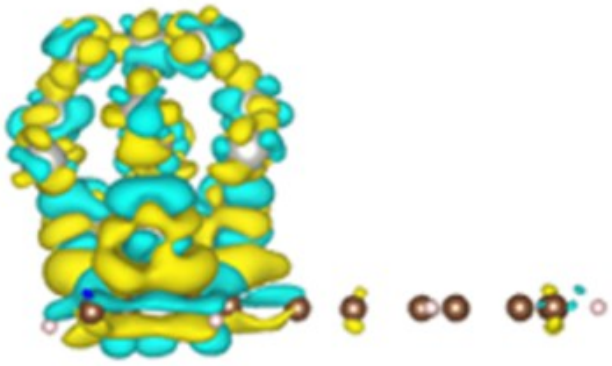

Figure S2. The electronic charge density difference for the Pd/HsGY system.

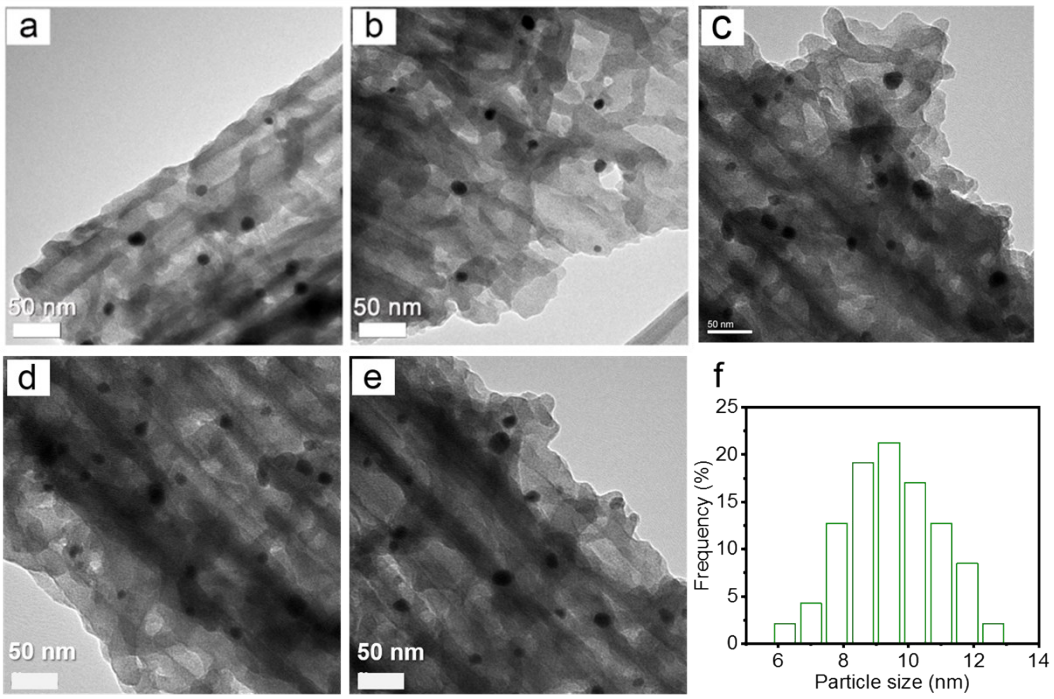

Figure S3. (a-e) TEM images of Pd/N-HsGY. (f) Histograms of size distribution of Pd nanoparticles.

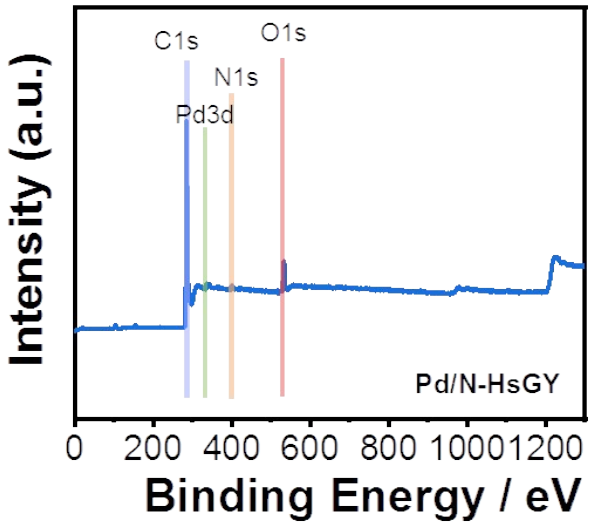

Figure S4. XPS full-scan spectra of Pd/N-HsGY.

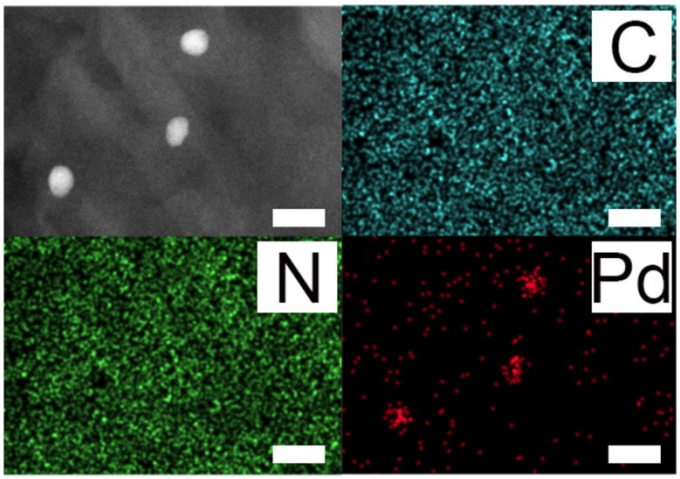

Figure S5. HRTEM mapping images of Pd/N-HsGY (bar = 20nm)

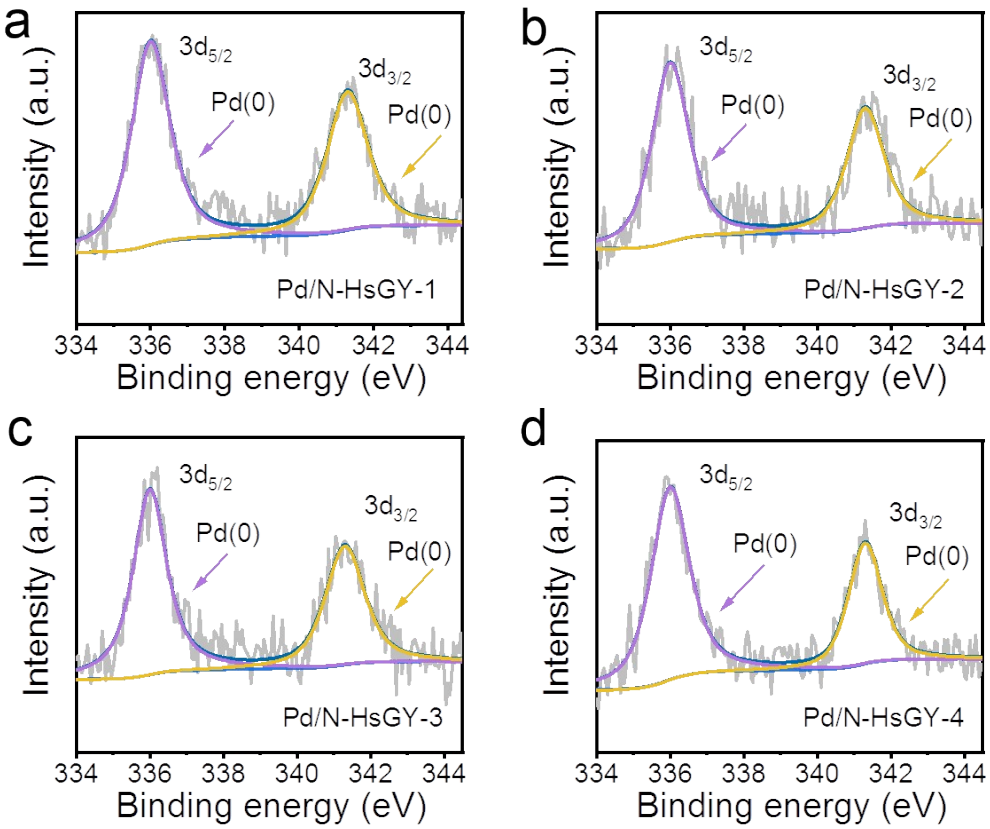

Figure S6. Pd 3d XPS spectra of several batches of Pd/N-HsGY (a) sample1, (b) sample2, (c) sample 3, and (d) sample 4.

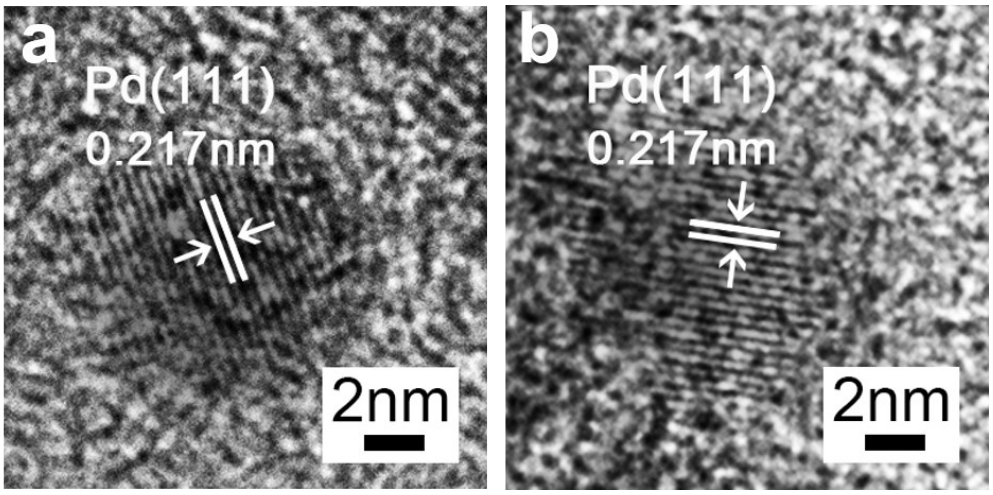

Figure S7 HRTEM images of (a) Pd/ HsGY and (b) Pd/N-HsGY.

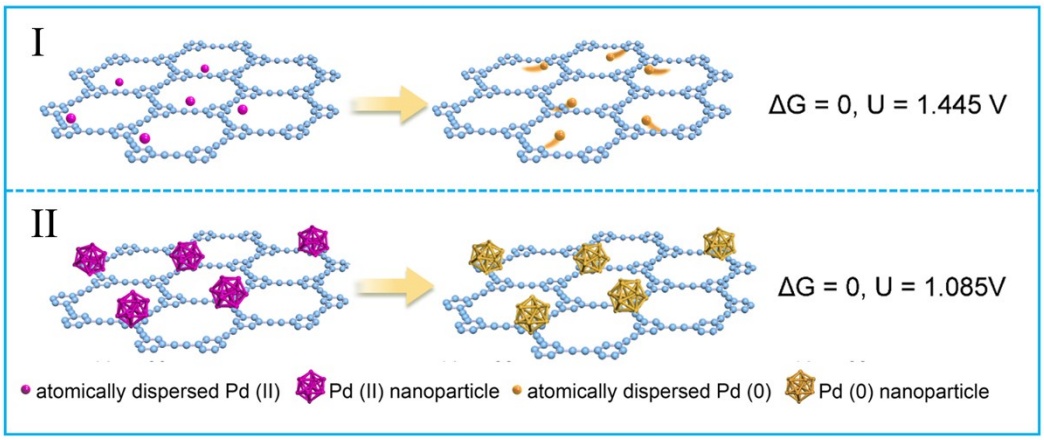

Figure S8. Calculation of redox potential of atomically dispersed Pd and Pd nanoparticle.

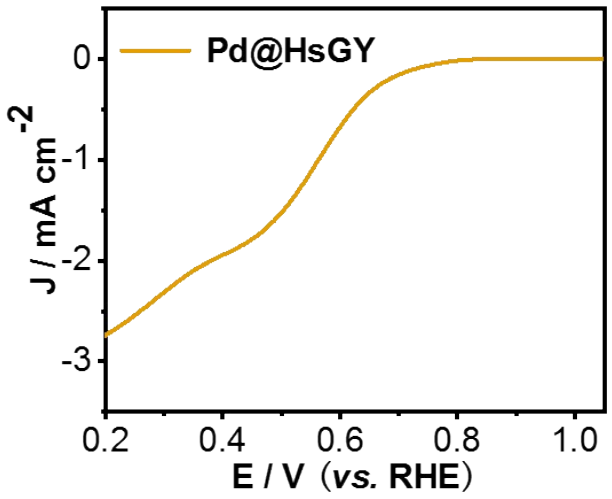

Figure S9. LSVs of Pd@HsGY in 0.1 M KOH.

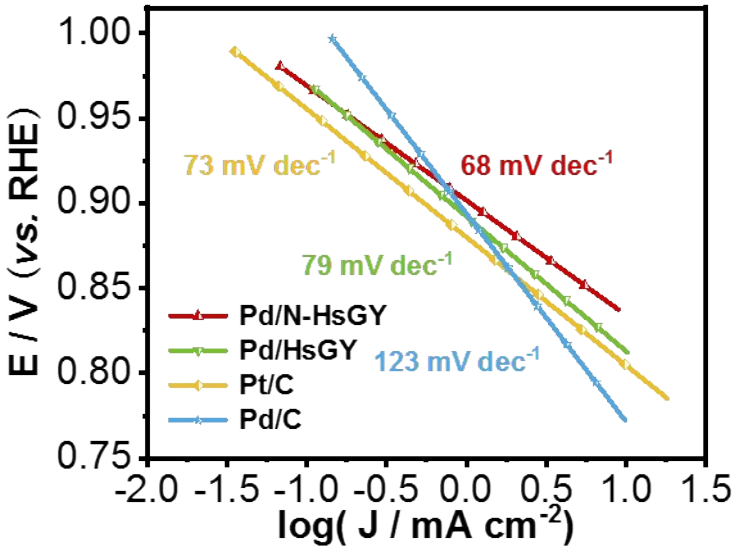

Figure S10. Corresponding Tafel plots of Pd/N-HsGY, Pd/HsGY, Pt/C, Pd/C in 0.1M KOH.

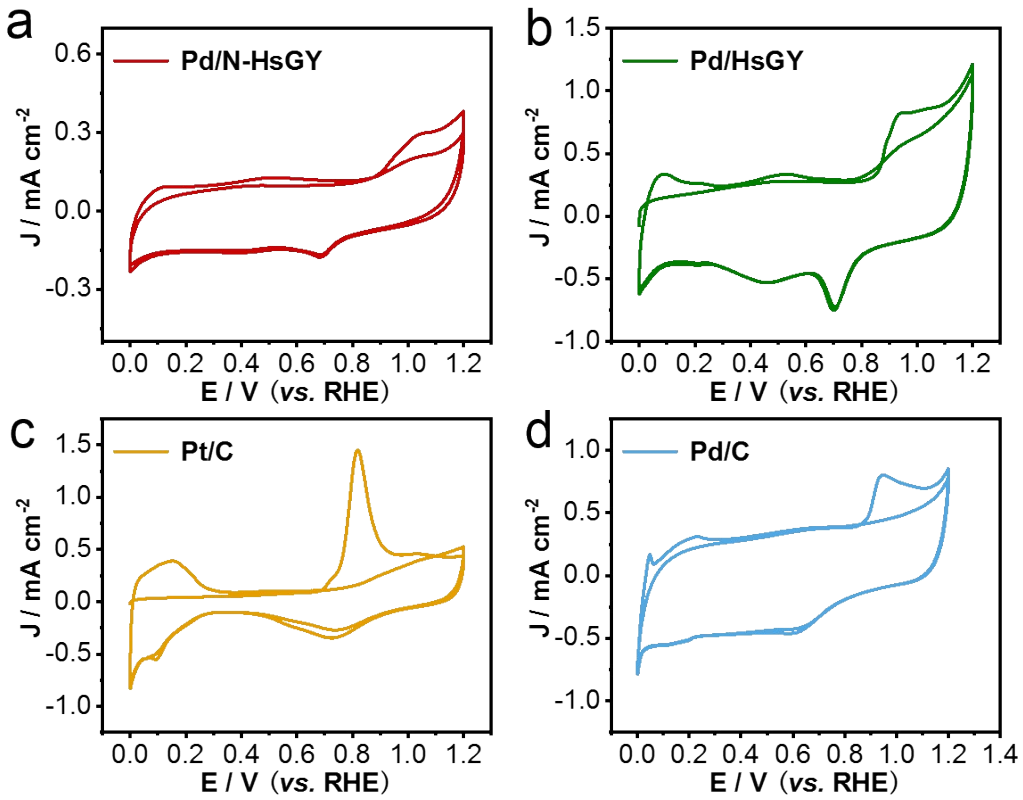

Figure S11. CO stripping voltammograms curves of (a) Pd/N-HsGY, (b) Pd/HsGY, (c) Pt/C, (d) Pd/C, respectively.

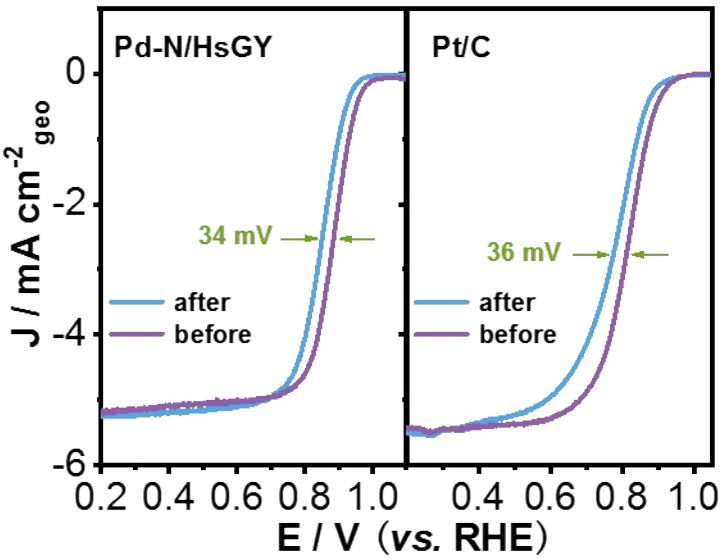

Figure S12. ORR polarization curves of Pd/N-HsGY and commercial Pt/C before and after before and after 5000 potential cycles in O_2-saturated 0.1 M KOH solution at 1600 rpm.

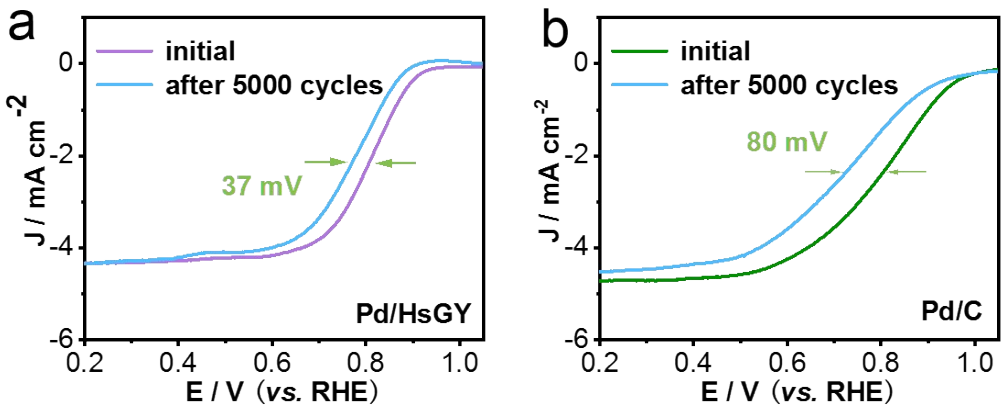

Figure S13. ORR polarization curves of (a) Pd/HsGY and (b) commercial Pd/C before and after before and after 5000 potential cycles in O_2-saturated 0.1 M KOH solution at 1600 rpm.

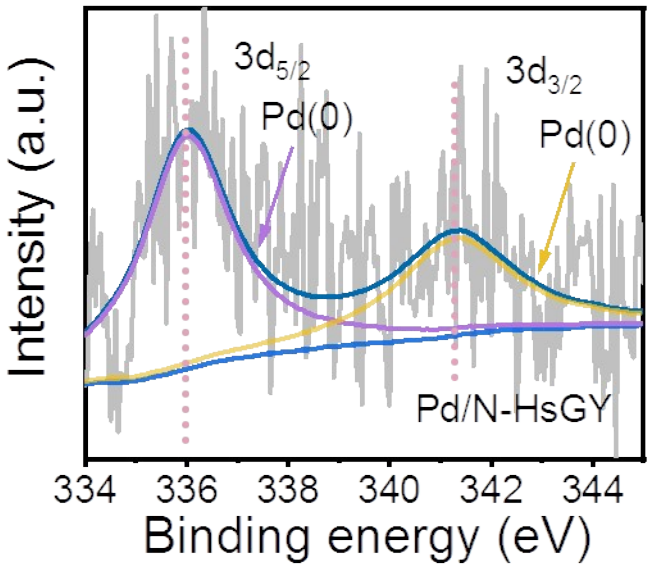

Figure S14. Pd 3d XPS spectra of Pd/N-HsGY after electrocatalytic test.

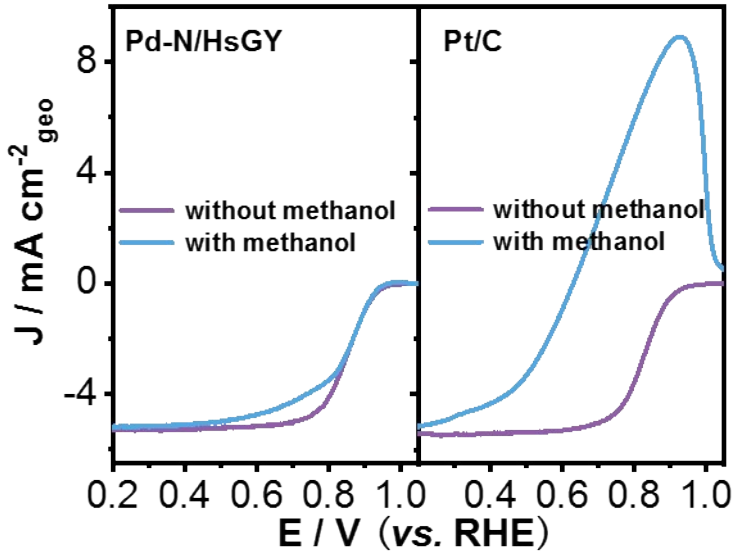

Figure S15. ORR polarization curves of Pd/N-HsGY and Pt/C before and after injecting methanol into O_2-saturated 0.1 M KOH at 1600 rpm. (h) Pd/N-HsGY in O_2-saturated 0.1 M KOH at various rotation speeds.

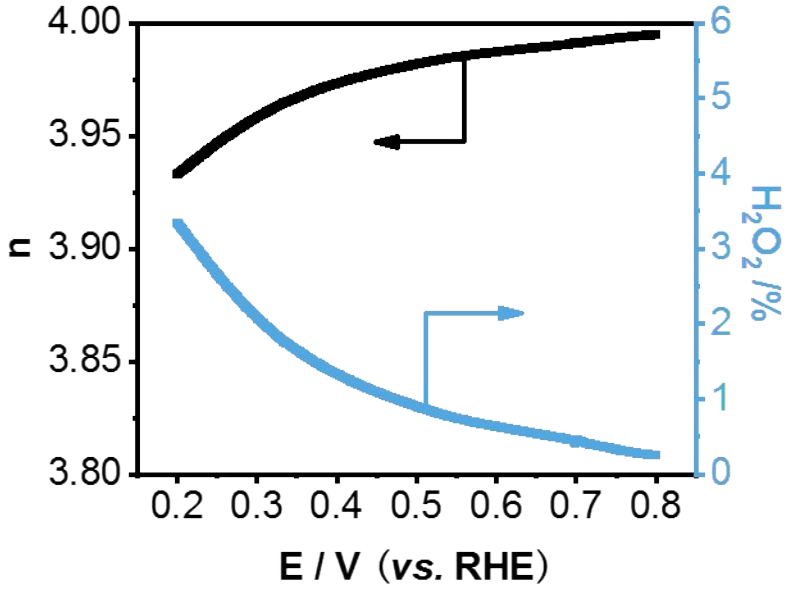

Figure S16. Electron transfer numbers and peroxide yields for Pd/N-HsGY in 0.1M KOH.

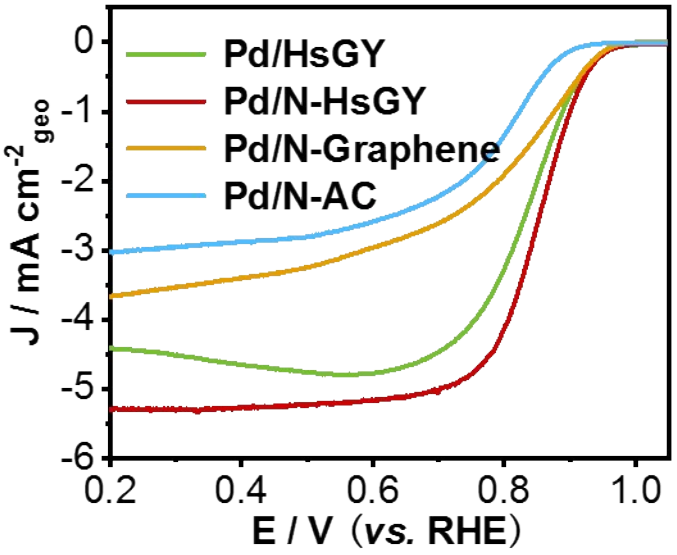

Figure S17. LSVs of Pd/HsGY, Pd/N-HsGY, Pd/N-graphene and Pd/N-AC in 0.1 M KOH.

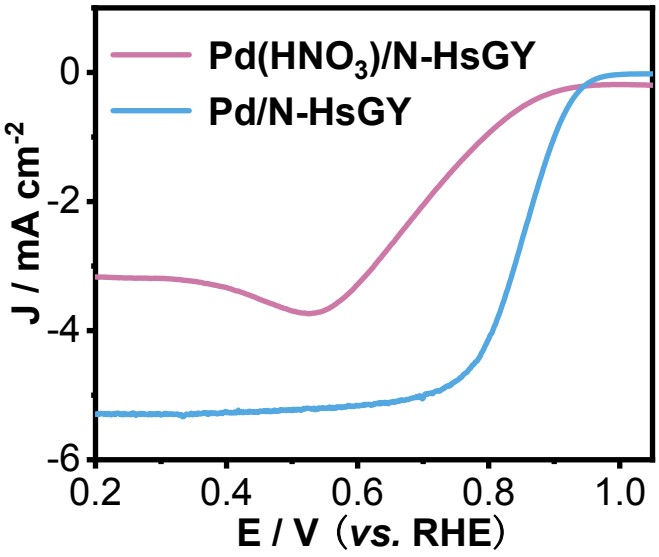

Figure S18. (a) Linear sweep voltammetry curves of Pd/N(HNO_3)-HsGY and Pd/N-HsGY under 0.1 M KOH at 1600rpm.

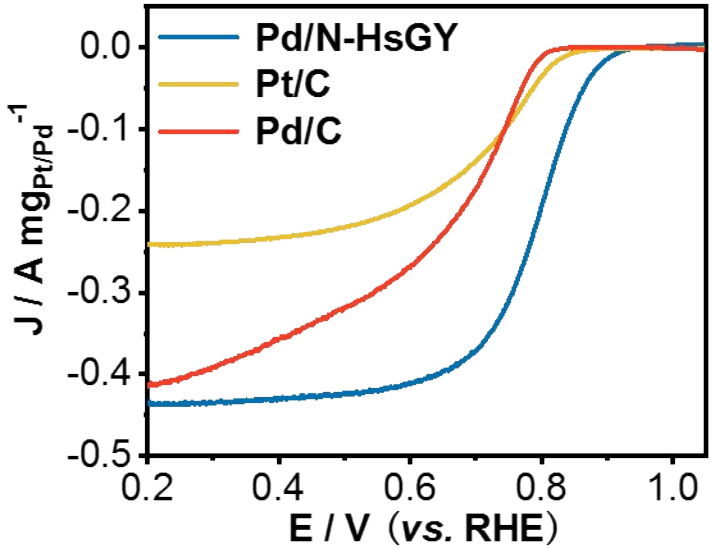

Figure S19. Mass activities of Pd/N-HsGY, commercial Pt/C and Pd/C in 0.1M $HClO_4$.

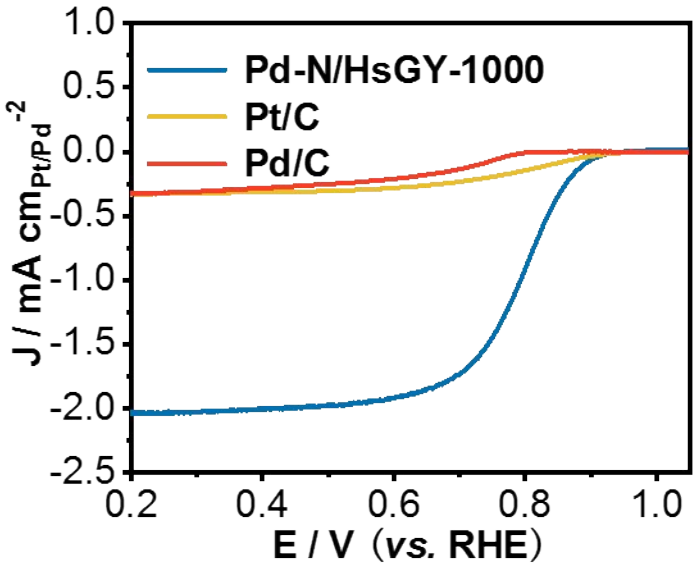

Figure S20. Specific activities of Pd/N-HsGY, commercial Pt/C and Pd/C in 0.1M $HClO_4$.

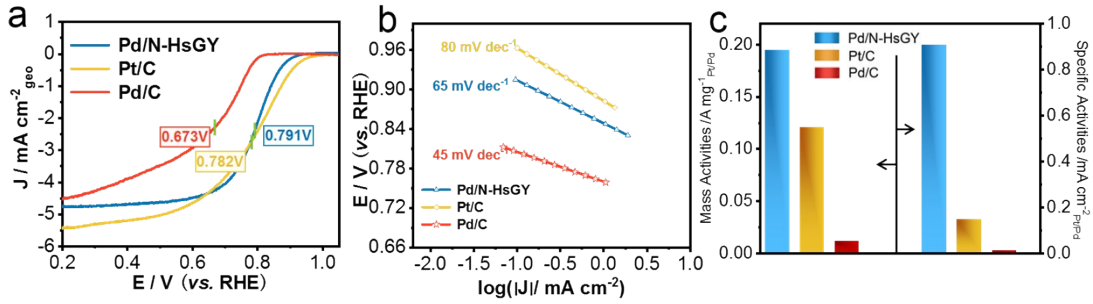

Figure S21. Performance of catalysts for the oxygen reduction reaction in acidic media. (a) Linear sweep voltammetry curves of Pd/N-HsGY, commercial Pt/C and Pd/C under acidic conditions at 1600 rpm. (b) Corresponding Tafel plots of Pd/N-HsGY, Pd/HsGY, Pt/C, Pd/C. (c) Specific and mass activities of the catalysts at 0.8 V.

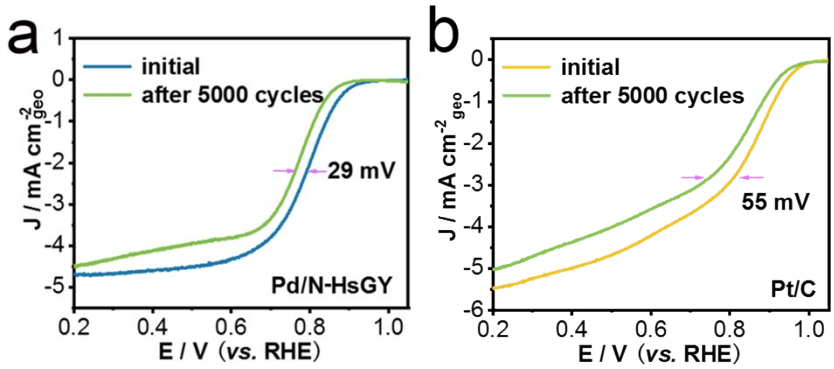

Figure S22. ORR polarization curves of (a) Pd/N-HsGY and (b) commercial Pt/C before and after injecting methanol into O_2-saturated 0.1 M $HClO_4$ at 1600 rpm.

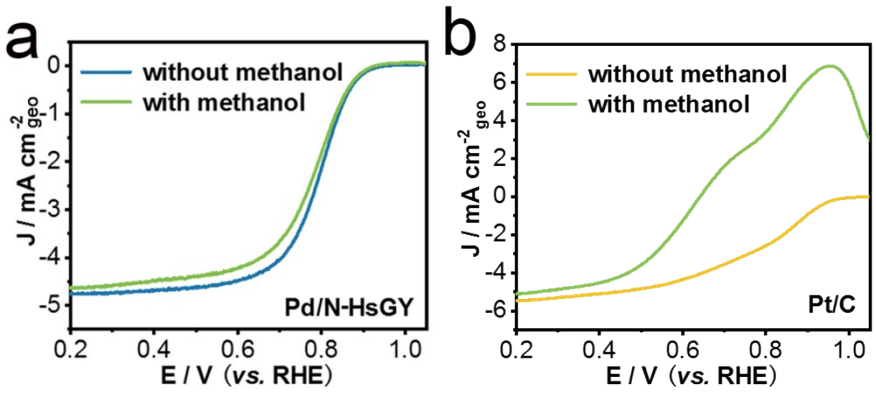

Figure S23. ORR polarization curves of (a) Pd/N-HsGY and (b) commercial Pt/C before and after 5000 potential cycles in O_2-saturated 0.1 M $HClO_4$ solution at 1600 rpm.

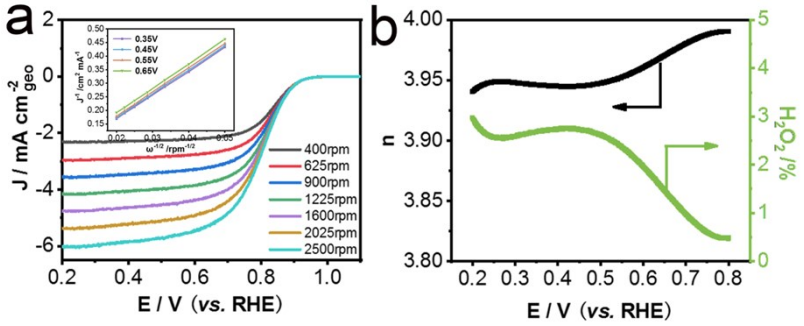

Figure S24. (a) Pd/N-HsGY in O_2-saturated 0.1 M $HClO_4$ at various rotation speeds. Inset: The K–L plots of Pd/N-HsGY. (b) Electron transfer numbers and peroxide yields for Pd/N-HsGY.

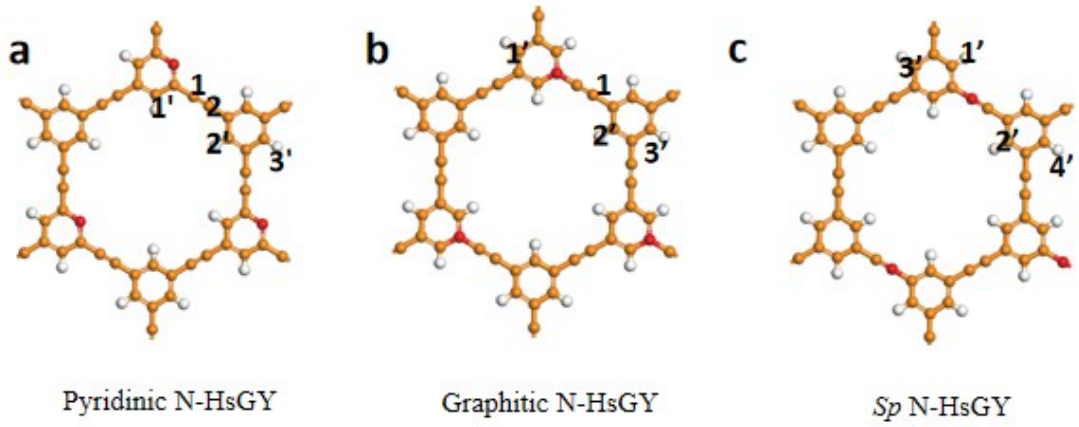

Figure S25. The fragment of N-HsGY system and the possible active sites for ORR were labeled with Arabic numbers: (a) Pyridinic-N (b) Graphitic-N (c) sp-N. (H atoms are white; C atoms are orange and N atoms are red).

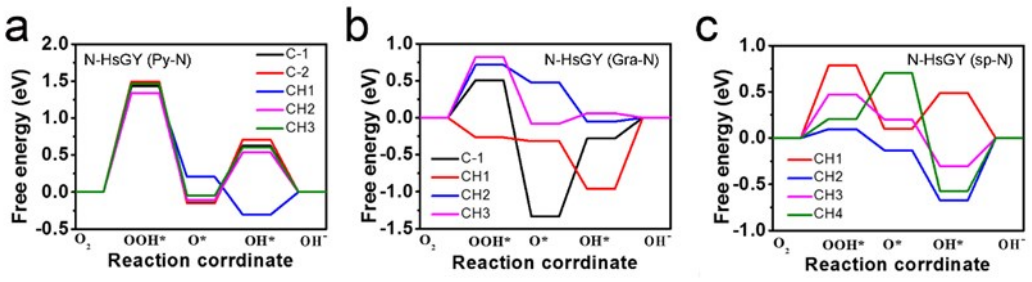

Figure S26. Free energy diagrams during the ORR for N-HsGY system: (a) Pyridinic-N (N-HsGY (Py-N)), (b) Graphitic-N (N-HsGY (Gra-N)) (c) sp-N (N-HsGY (sp-N)) under alkaline condition at potentials of 0.401 V

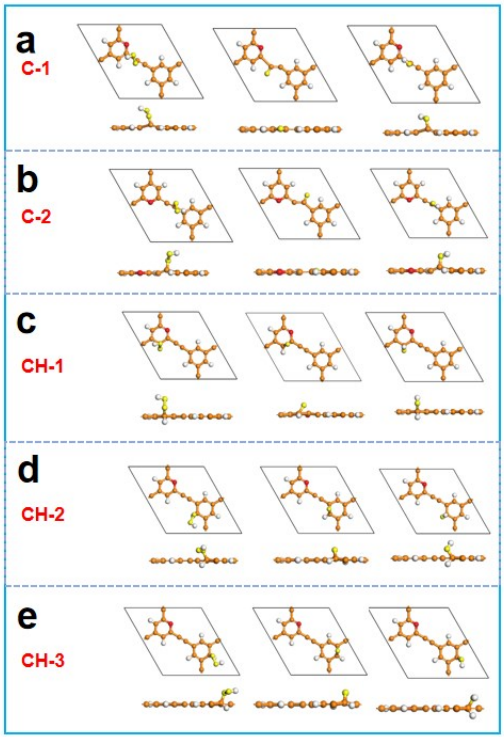

Figure S27. The optimized configurations of intermediate states (*OOH,*O or *OH) of Pyridinic-N-HsGY for site 1 (a), 2 (b), 1’ (c), 2’ (d) and 3’ (e). (H atoms are white; C atoms are orange and N atoms are red and O atoms are yellow).

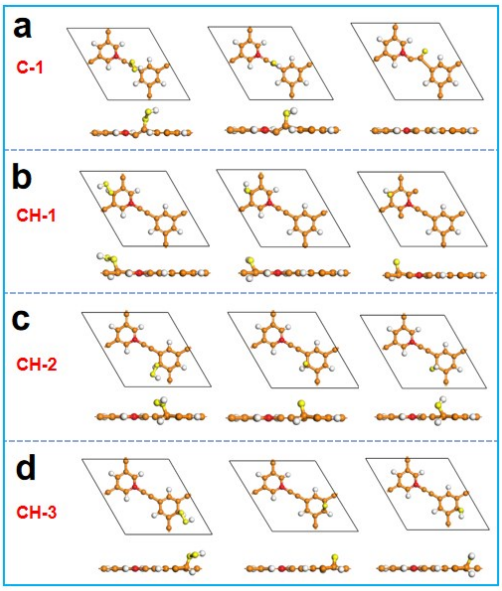

Figure S28. The optimized configurations of intermediate states (*OOH,*O or *OH) of Graphitic-N-HsGY for site 1 (a), 1' (b), 2' (c) and 3 (d). (H atoms are white; C atoms are orange and N atoms are red and O atoms are yellow).

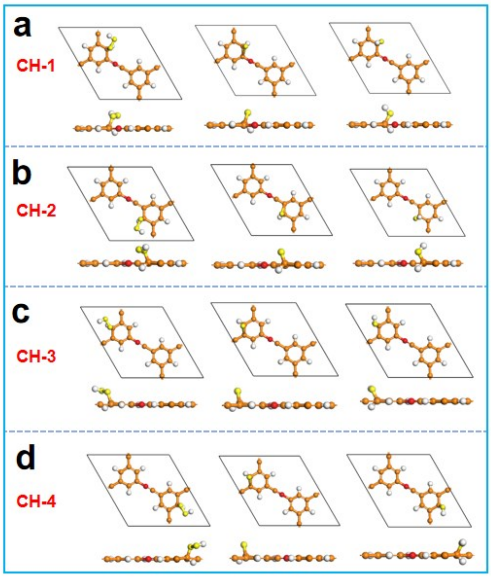

Figure S29. The optimized configurations of intermediate states (*OOH, *O or *OH) of sp-N-HsGY for site 1' (a), 2'(b), 3'(c) and 4'(d). (H atoms are white; C atoms are orange and N atoms are red and O atoms are yellow).

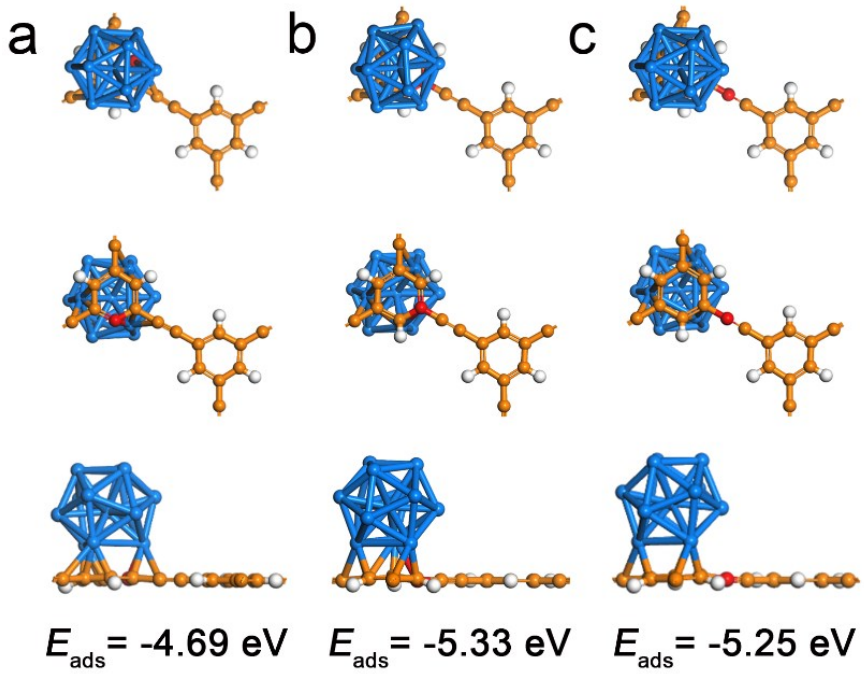

Figure S30. The optimized configurations for Pd/N-HsGY system and its adsorption energy. (a) Pyridinic-N (b) Graphitic-N (c) sp-N. (1: top views, 2: bottom views, 3: side views; H atoms are white; C atoms are orange; N atoms are red and Pd atoms are blue).

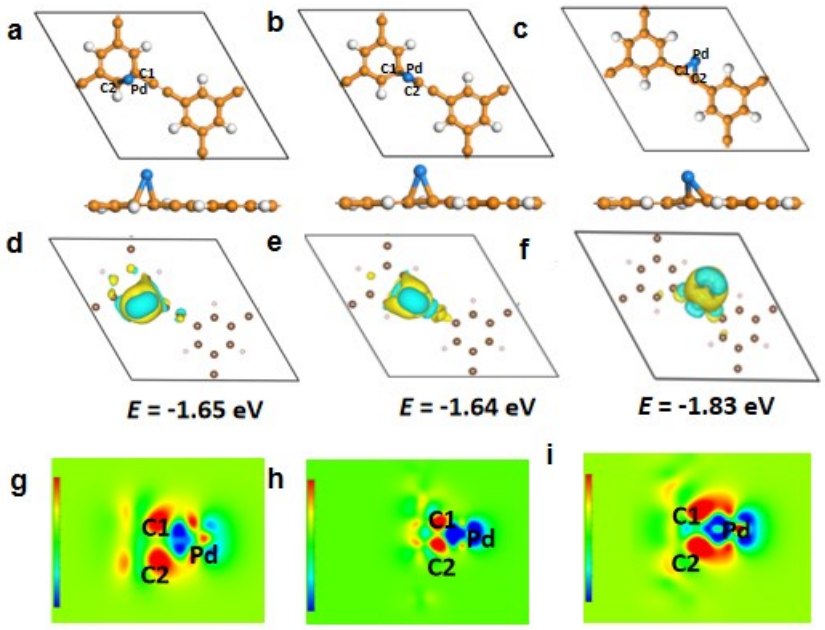

Figure S31. (a-c) The different configurations for single Pd atom within the HsGY system. The H atoms are white; C atoms are origin and Pd atoms are blue. **(**d-i) The electronic charge density difference for the single Pd atom on HsGY and the adsorption energy is listed. The accumulation and loss of the charge are represented by yellow and blue regions, respectively.

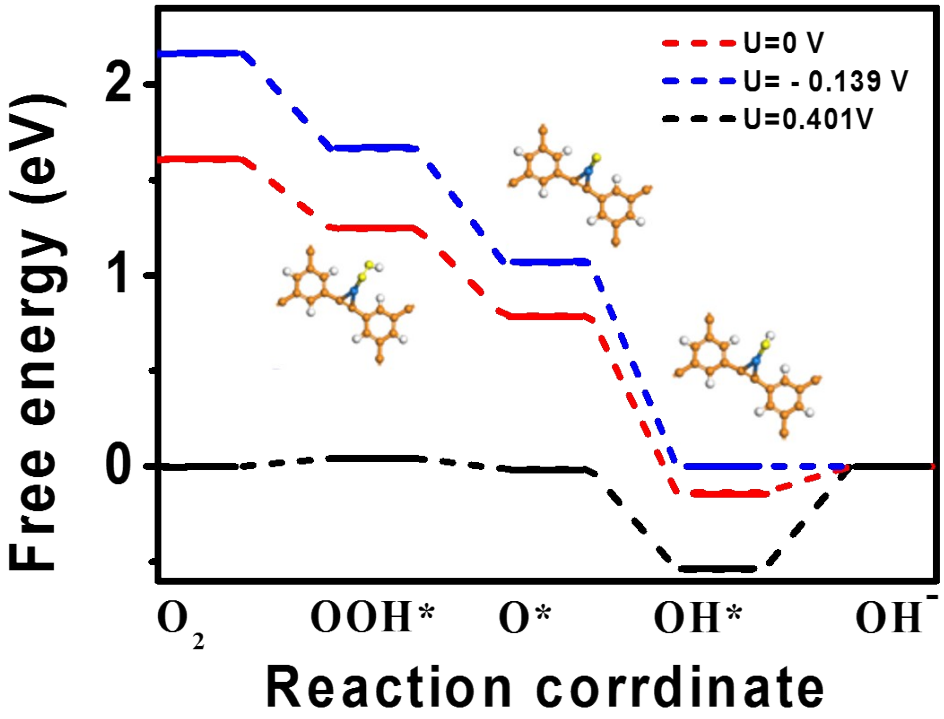

Figure S32. The free energy diagram during the ORR for single Pd atom on HsGY under acidic condition at different potentials. The optimized configurations are listed. (H atoms are white; C atoms are orange; O atoms are yellow and Pd atoms are blue).

Table S1 Comparison of some advanced Pd doped noble metal ORR catalysts in 0.1 M KOH electrolyte.

Catalyst	**Limited current density (mA cm^{-2})**	**Half-wave potential (V *vs.* RHE)**	**Onset potential (V *vs.* RHE)**	**Reference**
Pd/N-HsGY	**5.3**	**0.849**	**0.96**	**This work**
rGO/Cu_3Pd	5	0.835	0.9	Small 2020, 1907341.
HsGDY/Cu_3Pd-750	5.8	0.87	0.94	Small 2020, 1907341.
PdCo-300	5.1	0.83	0.93	Appl. Catal. B-Environ. 2019, 243, 175-182.
FFPC/NPCNFs-3	5.25	0.79	0.91	Small 2019, 1805032.
Pd/MnO_2-CNT	6.5	0.695	0.85	J. Mater. Chem. A, 2018, 6, 23366.
$Pd_{50}Cu_{50}$	5.2	0.87	0.95	Nat. Commun. 2018 9, 3702.
Pd@PdO-Co_3O_4	4.9	0.755	0.88	Adv. Energy Mater. 2017, 1702734.
Pd/NG	6.8	0.80	0.94	ACS Appl. Mater. Interfaces 2018, 10, 18734-18745.
fct-PdFe@Pd@NG	8.1	0.83	0.96	ACS Appl. Mater. Interfaces 2018, 10, 18734-18745.
$MnPd_3$/C NHs	5.3	0.78	0.9	ACS Appl. Mater. Interfaces 2018, 10, 8155−8164.

Table S2 The CO oxidation peak area and the ECSA data of the catalysts.

	S_{CO} (mA·V)	*ECSA* ($m^2/g_{Pt/Pd}$)
Pd/N-HsGY	0.00249	21.6
Pd/ HsGY	0.00618	53.5
Pt/C	0.01733	82.8
Pd/C	0.01453	126.3

Table S3 Contents (at%) of Pd in Pd 3d XPS spectra.

Sample	Pd (at%)
Pd/N-HsGY	0.91
Pd(HNO3)/N-HsGY	0.25

1. Fang, Y.; Xue, Y.; Hui, L.; Yu, H.; Liu, Y.; Xing, C.; Lu, F.; He, F.; Liu, H.; Li, Y., In situ growth of graphdiyne based heterostructure: Toward efficient overall water splitting. *Nano Energy* **2019,** *59*, 591-597.
2. Lv, Q.; Si, W.; He, J.; Sun, L.; Zhang, C.; Wang, N.; Yang, Z.; Li, X.; Wang, X.; Deng, W.; Long, Y.; Huang, C.; Li, Y., Selectively nitrogen-doped carbon materials as superior metal-free catalysts for oxygen reduction. *Nature communications* **2018,** *9* (1), 3376.
3. He, Z.; Dong, B.; Wang, W.; Yang, G.; Cao, Y.; Wang, H.; Yang, Y.; Wang, Q.; Peng, F.; Yu, H., Elucidating Interaction between Palladium and N-Doped Carbon Nanotubes: Effect of Electronic Property on Activity for Nitrobenzene Hydrogenation. *ACS Catal.* **2019,** *9* (4), 2893-2901.
4. Zhao, Y.; Yang, N.; Yao, H.; Liu, D.; Song, L.; Zhu, J.; Li, S.; Gu, L.; Lin, K.; Wang, D., Stereodefined Codoping of sp-N and S Atoms in Few-Layer Graphdiyne for Oxygen Evolution Reaction. *J. Am. Chem. Soc.* **2019,** *141* (18), 7240-7244.